The unique trimeric assembly of the virulence factor HtrA from *Helicobacter pylori* occurs via N-terminal domain swapping

Received for publication, January 5, 2019, and in revised form, March 27, 2019 Published, Papers in Press, April 1, 2019, DOI 10.1074/jbc.RA119.007387

Zhemin Zhang[‡1], Qi Huang[‡1], Xuan Tao[‡], Guobing Song[§], Peng Zheng[§], Hongyan Li[¶], Hongzhe Sun[¶], and Wei Xia[‡2]

From the [‡]MOE Key Laboratory of Bioinorganic and Synthetic Chemistry, School of Chemistry, Sun Yat-sen University, Guangzhou, 510275, China, the [¶]Department of Chemistry, University of Hong Kong, Pokfulam Road, Hong Kong SAR, China, and the [§]State Key Laboratory of Coordination Chemistry, School of Chemistry and Chemical Engineering, Nanjing University, Nanjing 210023, China

Edited by Wolfgang Peti

Knowledge of the molecular mechanisms of specific bacterial virulence factors can significantly contribute to antibacterial drug discovery. *Helicobacter pylori* is a Gram-negative microaerophilic bacterium that infects almost half of the world's population, leading to gastric disorders and even gastric cancer. *H. pylori* expresses a series of virulence factors in the host, among which high-temperature requirement A (*Hp*HtrA) is a newly identified serine protease secreted by *H. pylori*. *Hp*HtrA cleaves the extracellular domain of the epithelial cell surface adhesion protein E-cadherin and disrupts gastric epithelial cell junctions, allowing *H. pylori* to access the intercellular space. Here we report the first crystal structure of *Hp*HtrA at 3.0 Å resolution. The structure revealed a new type of HtrA protease trimer stabilized by unique N-terminal domain swapping distinct from other known HtrA homologs. We further observed that truncation of the N terminus completely abrogates *Hp*HtrA trimer formation as well as protease activity. In the presence of unfolded substrate, *Hp*HtrA assembled into cage-like 12-mers or 24-mers. Combining crystallographic, biochemical, and mutagenic data, we propose a mechanistic model of how *Hp*HtrA recognizes and cleaves the well-folded E-cadherin substrate. Our study provides a fundamental basis for the development of anti-*H. pylori* agents by using a previously uncharacterized HtrA protease as a target.

The current paradigm for treatment of bacterial infection is to eradicate bacterial pathogens with antibiotics. However, rapid evolution and dissemination of antibiotic resistance among pathogens pose a huge threat to human health worldwide (1). Recently, antivirulence strategies have been proposed as an alternative for the development of new antimicrobials (2, 3). The strategy seeks to interfere with the bacterial virulence factors that promote infection without threatening their existence. This leads to reduced selective pressure for drug-resistant mutations. Notably, development of antivirulence drugs requires an in-depth understanding of the structures and functions of virulence factors in disease processes.

Helicobacter pylori, a Gram-negative microaerophilic bacterium that colonizes the human stomach and is the leading cause of human gastric disease, such as peptic ulcers, gastritis, and even gastric cancer (4), produces a series of virulence factors, *e.g.* the oncoprotein CagA (5), the vacuolating cytotoxin VacA (6), and urease enzyme (7). Some virulence factors have been recognized as potential drug targets to eradicate *H. pylori* infection (8, 9). High-temperature requirement A protein of *H. pylori* (*Hp*HtrA) is a newly identified virulence factor that helps *H. pylori* to efficiently break through the gastric epithelium by cleaving proteins within the epithelial tight junction (occludin and claudin-8) and adherens junction (E-cadherin) (10, 11). Structural and functional characterization of this virulence factor may facilitate the design of new types of anti-*H. pylori* drugs.

HtrA homologs, which are widely found in prokaryotic and eukaryotic organisms, represent a class of highly evolutionarily conserved heat shock–induced serine proteases and chaperones (12–14). HtrA proteases are composed of an N-terminal signal peptide, a trypsin-like serine protease core domain, and a C-terminal PDZ (15) domain. Based on the different domain organization, HtrA family proteins can be classified into three groups. The members in group 1 contain only one protease and one PDZ domain, such as *Escherichia coli* DegS (*Ec*DegS) and HtrA2 in mammals (16, 17). Proteins in group 2 have one protease domain and two PDZ domains, including *Hp*HtrA, *E. coli* DegP (*Ec*DegP), and *E. coli* DegQ (*Ec*DegQ) (18, 19). Those in group 3 contain two protease domains and four PDZ domains, such as the recently reported Nma111p (20). *Ec*DegP is a well-characterized group 2 protease. Crystal structures revealed that the inactive *Ec*DegP is a hexamer. The basic *Ec*DegP trimeric

This work was supported by grants from the National Natural Science Foundation of China (21671203, 21771103, and 21877131); the Science and Technology Program of Guangzhou, China (201707010038); RGC of Hong Kong (17305415, 17333616, and 17307017); the Ministry of Education of China (IRT-17R111); Fundamental Research Funds for the Central Universities, Natural Science Foundation of Jiangsu Province (BK20160639); the Shuangchuang Program of Jiangsu Province; and startup funding from Sun Yat-sen University. The authors declare that they have no conflicts of interest with the contents of this article.

This article contains Figs. S1–S11, Tables S1 and S2, Methods, and References.

The atomic coordinates and structure factors (codes 5Y2D and 5Y38) have been deposited in the Protein Data Bank (http://wwpdb.org/).

[1] These authors contributed equally to this work.

[2] To whom correspondence should be addressed. Tel.: 86-20-84111503; E-mail: xiawei5@mail.sysu.edu.cn.

unit is composed of three monomers that closely interact with each other using the protease domains (21, 22). The trimer was further assembled into a hexamer in a manner of staggered dimers of trimers (23, 24). When it engages with the proper substrates, *Ec*DegP forms a higher-order multimer and exhibits protease activity (18, 22, 25, 26).

It is known that HtrA family proteases strictly act in the periplasm and play a vital role in protein quality control (27, 28). However, recent studies demonstrated that *H. pylori* actively secretes HtrA into the extracellular environment, where it cleaves the extracellular domain of the epithelial cell surface adhesion protein E-cadherin, facilitating *H. pylori* transmigration across gastric epithelial cells (29–32). HtrA in *H. pylori* contains a signal peptide that is important for Sec-dependent cleavage and transport of the protease across the inner membrane into the periplasm (13, 14, 27, 33). Although HtrA has been reported to be enriched in *H. pylori* outer membrane vesicles, the detailed mechanism of how it is transported across the outer membrane remains unclear (34). E-cadherin is a single-transmembrane protein consisting of five extracellular (EC) domains,[3] an intracellular domain, and a transmembrane domain (35). EC domains adopt a calcium-dependent homophilic interaction to mediate intercellular adhesion between epithelial cells (36). Edman degradation and mass spectrometry–based proteomics demonstrated that the [VITA]-[VITA]*XX*D[DN] signature motifs located at the linker regions of the EC domains are preferentially cleaved by *Hp*HtrA (37). Importantly, inhibition of *Hp*HtrA activity by chemical compounds efficiently blocked *H. pylori* transmigration across the gastric epithelial barrier (38, 39). Moreover, generation of an *htrA* knockout mutant in *H. pylori* is fatal, implying that *Hp*HtrA is critical for *H. pylori* survival (40, 41). Therefore, *Hp*HtrA has been considered a potential attractive drug target, given its vital role in the pathogenesis and survival of *H. pylori* (42).

Here we report the crystal structure of HtrA from *H. pylori*. The structure reveals a trimeric *Hp*HtrA containing a unique extended N terminus that is absent in other HtrA homologs. Importantly, the N terminus bridges HtrA monomers through domain swapping to stabilize the homotrimer, which has not been identified in other HtrA homologs reported so far. We further demonstrate that the N terminus is also essential for *Hp*HtrA oligomer assembly and protease activity. Moreover, a key residue, Lys^{328}, in the *Hp*HtrA PDZ1 domain was identified to be essential for E-cadherin cleavage but is dispensable for unstructured β-casein substrate. All of these data reveal a novel type of HtrA family protease secreted by the human pathogen *H. pylori*.

Results

The N terminus of HpHtrA is critical for protease activity

Sequence alignments of HtrA homologs from different bacterial species show that *Hp*HtrA has almost the same domain composition as other members, including a signal peptide, a protease domain, and two PDZ domains (Fig. 1*A*). However, *Hp*HtrA has a relatively extended N-terminal region that contains 19 residues after the signal peptide (^{18}GNIQIQSMPKVKERVSVDP^{35}) (Fig. 1*B*). To investigate the function of each domain, a series of domain truncation mutants of *Hp*HtrA was constructed and purified (Fig. S1), including a mutant with the N-terminal 19 residues truncated (*Hp*HtrA-ΔN), a mutant with the PDZ2 domain truncated (*Hp*HtrA-ΔPDZ2), and a mutant with both PDZ domains truncated (*Hp*HtrA-ΔPDZ1–2). The protease activity of the mutants was measured using a nonspecific substrate, β-casein, as described previously (32). As shown in Fig. 1*C*, proteolytic activity of the *Hp*HtrA-ΔPDZ1–2 mutant was completely abolished. In contrast, the *Hp*HtrA-ΔPDZ2 mutant exhibited even higher protease activity compared with the WT *Hp*HtrA (residues from Gly^{18} to Lys^{475} without the signal peptide). The results are consistent with previous reports showing that the PDZ1 domain is essential for protease activity and responsible for recognizing and sequestering unfolded substrates through C-terminal residues, whereas the PDZ2 domain is mostly involved in maintaining the hexameric cage of DegP and displays an inhibitory role in chaperone and protease activity (18, 43, 44). Intriguingly, removal of the short N terminus also abrogated *Hp*HtrA protease activity, indicative of an essential role of the N terminus in *Hp*HtrA protease activity. The proteolytic activity of the mutants was subsequently measured using E-cadherin as a substrate. In contrast, all mutants showed decreased proteolytic activity against E-cadherin compared with WT *Hp*HtrA, implying that all of these domains might participate in the E-cadherin cleavage process (Fig. 1*D*).

The N terminus stabilizes the trimeric form of HpHtrA

In the absence of substrate, two *Ec*DegP trimers stack face to face to form an inactive hexamer (23); *Ec*DegS and *Ec*DegQ, two extensively studied HtrA family proteins in *E. coli*, were identified as homotrimers (19, 45). To characterize the conformational state of *Hp*HtrA in the absence of substrate, the oligomerization states of WT-*Hp*HtrA and different mutants were examined by size-exclusion chromatography. As shown in Fig. 2*A*, WT *Hp*HtrA was eluted at 11.5 ml with a calculated molecular mass of 170 kDa, consistent with a trimeric form of *Hp*HtrA (52 kDa for a monomer). *Hp*HtrA-ΔPDZ2 and *Hp*HtrA-ΔPDZ1–2 were both eluted as trimers with calculated molecular masses of 120 and 90 kDa, respectively. Unexpectedly, *Hp*HtrA-ΔN was eluted at 14.9 ml with a molecular mass of 50 kDa, indicative of a monomeric state of the *Hp*HtrA-ΔN mutant. It has been reported that an autoproteolytic process that results in cleavage of the N-terminal region of *Ec*DegP led to destabilization of a hexamer and formation of a monomer of *Ec*DegP (46). However, the autocleavage process removed the N-terminal 60–80 residues of *Ec*DegP, in contrast to truncation of the N-terminal 19 residues in *Hp*HtrA. The results indicate that the N terminus is essential to stabilize the *Hp*HtrA trimer. On the other hand, the trimeric form of HtrA is likely the minimal functional unit with prominent protease activity because activation of HtrA required the substrate sensor loop from one monomer to interact with the activation loop of a neighboring monomer (28, 47). Therefore, truncation of the N terminus of *Hp*HtrA disrupted its trimeric form and significantly abolished its protease activity.

[3] The abbreviations used are: EC, extracellular; AFM, atomic force microscopy.

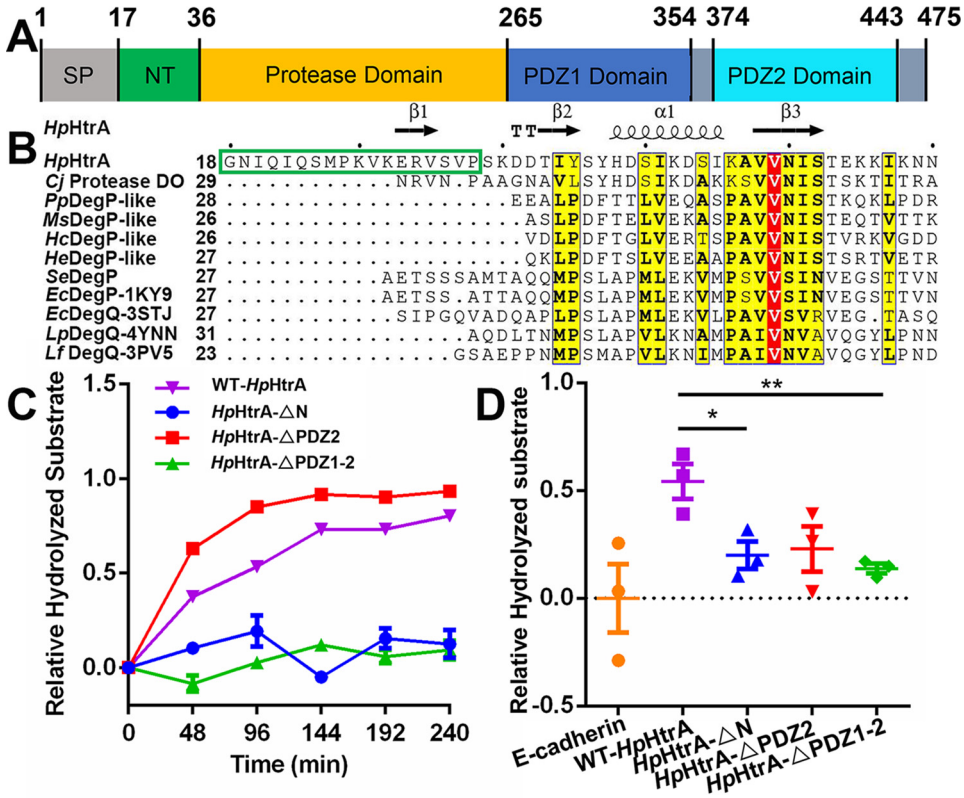

Figure 1. The N terminus of *Hp*HtrA is critical for protease activity. *A*, schematic of the *Hp*HtrA domain architecture. *SP*, signal peptide; *NT*, N terminus. *B*, sequence alignments of HtrA family proteins from different bacterial species. Identical or similar amino acids are highlighted. The secondary structure of *Hp*HtrA is shown. The *green box* indicates the extra N terminus of *Hp*HtrA. The abbreviated species names and their GenBank accession numbers and PDB codes are as follows: *Cj Protease DO*: *C. jejuni* serine protease Do (CAL35343); *PpDegP-like*: *Pseudomonas putida* DegP-like protein (B1J4D7); *MsDegP-like*: *Marinomonas* sp. DegP-like protein (A6VUA4); *HcDegP-like*: *Hahella chejuensis* DegP-like protein (Q2SL36); *HeDegP-like*: *Halomonas elongata* DegP-like protein (E1V4H2); *SeDegP*: *Salmonella enterica* DegP (P26982); *EcDegP-1KY9*: *E. coli* DegP (P0C0V0), PDB code 1KY9; *EcDegQ-3STJ*: *E. coli* DegQ (P39099), PDB code 3STJ; *LpDegQ-4YNN*: *Legionella pneumophila* DegQ (Q5ZVV9), PDB code 4YNN; *LfDegQ-3PV5*: *Legionella fallonii* DegQ (CEG56683), PDB code 3PV5. *C*, time-course β-casein cleavage assay of WT *Hp*HtrA and mutants. The total amount of β-casein substrate was normalized as 1.0, and the hydrolyzed substrates are plotted against reaction time. *D*, E-cadherin cleavage assay of WT-*Hp*HtrA and mutants. The total amount of E-cadherin in each reaction was normalized as 1.0, and hydrolyzed substrate after 12 h is plotted. All cleavage experiments were done in triplicate, and the results are shown as the mean with standard deviation. *, $p < 0.05$; ** $p < 0.01$.

Structural characterization of HpHtrA

To further understand how the N terminus stabilizes trimeric *Hp*HtrA, we first determined the crystal structure of full-length WT *Hp*HtrA at a resolution of 3.7 Å (PDB code 5Y2D). The full-length WT *Hp*HtrA crystals grew in trigonal space group *R*32 and contained one monomeric *Hp*HtrA molecule per asymmetric unit. In the full-length *Hp*HtrA structure, only the protease and PDZ1 domain are well defined with clear electronic density, whereas the PDZ2 domain is partially visible (Fig. 2*B*). Intriguingly, weak but evident electron density was observed for the extended N terminus of *Hp*HtrA, which is usually disordered and invisible in other HtrA homolog structures (22, 23, 26, 47, 48).

To obtain a structure with higher resolution, we crystallized *Hp*HtrA-ΔPDZ2. The *Hp*HtrA-ΔPDZ2 structure was solved by molecular replacement and refined to 3.0 Å resolution (PDB code 5Y28). The crystal form belongs to the orthorhombic *P*222 space group and contains one *Hp*HtrA-ΔPDZ2 trimeric molecule per asymmetric unit. In this structure, each *Hp*HtrA monomer is composed of a protease domain and a C-terminal PDZ1 domain. However, only two PDZ1 domains are visible with clear electron densities among three *Hp*HtrA monomers. Typically, *Hp*HtrA monomers are packed symmetrically around a 3-fold molecular axis as a funnel-like shape, with the protease domain forming the core and the PDZ1 domain extending outward (Fig. 2*C*). The *Hp*HtrA protease domain is similar to other proteases of the trypsin family, with two perpendicular β barrel lobes and a C-terminal α helix. The backbone root mean square deviation between the *Ec*DegP and *Hp*HtrA protease domains is 0.83 Å. The catalytic triad is located in a crevice between two β barrel lobes, including residues His^{116}, Asp^{147}, and Ser^{221} (Fig. 2*D*). The relative orientation between the PDZ1 and protease domains is almost the same in both full-length *Hp*HtrA and *Hp*HtrA-ΔPDZ2 structures (Fig. S2). It has been reported that the PDZ1 domain tilts away from the protease domain upon *Ec*DegP activation. Structural alignments of *Hp*HtrA with inactive (PDB code 1KY9) and active (PDB code 3CS0) *Ec*DegP demonstrate that the overall conformation of *Hp*HtrA protease and the PDZ1 domain is identical to the inactive form, with a root mean square deviation of all Cα atoms of 1.6 Å (Fig. S1).

Intriguingly, the N-terminal region of *Hp*HtrA (Gly^{18}-Tyr^{44}) has clear electron density in all *Hp*HtrA-ΔPDZ2 monomers, which allows the N terminus model to be built unambiguously (Fig. S3). The N terminus of *Hp*HtrA is stretching out from the protease domain and is mainly composed of two short β strands and two unstructured loop regions: loop1 (Gln^{21}-Lys^{29}), β1

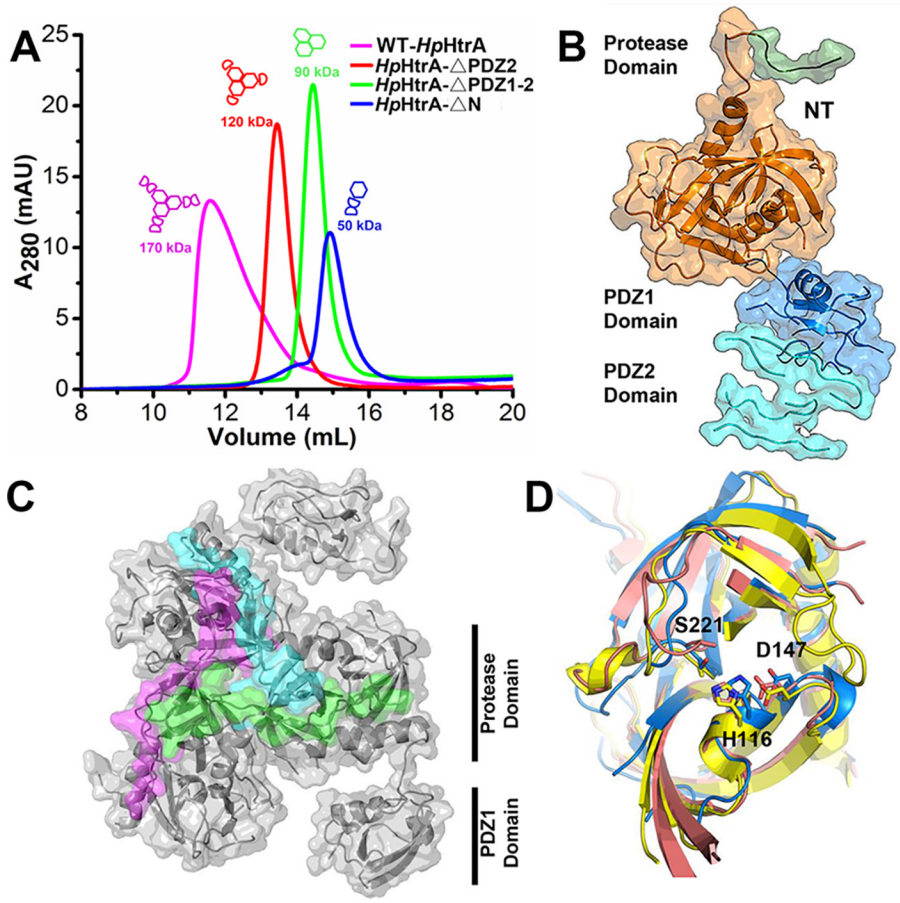

Figure 2. Crystal structure of *Hp*HtrA. *A*, size-exclusion chromatography analysis of WT *Hp*HtrA and mutants. The schematics and molecular masses for each sample are shown. *mAU*, milli-absorbance units. *B*, overall structure of the full-length WT *Hp*HtrA monomer. The N terminus (*NT*), protease domain, and PDZ1 and PDZ2 domains are shown as cartoons, and surfaces are colored in *green*, *orange*, *marine*, and *cyan*, respectively. *C*, the overall structure of the *Hp*HtrA-ΔPDZ2 trimer. Each chain is shown as a cartoon and surface, with the NT in different colors. *D*, HtrA protease domain. The protease domains of *Hp*HtrA-ΔPDZ2 (*marine*), inactive *Ec*DegP (*deep salmon*, PDB code 1KY9), and active *Ec*DegP (*yellow*, PDB code 3CS0) are superimposed and shown as cartoons. The conserved residues of the catalytic triad of HtrA are shown as *sticks* and numbered according to the *Hp*HtrA sequence.

(Glu^{30}-Val^{32}), β2 (Thr^{40}-Ser^{43}), and loop2 (Ser^{33}-Asp^{39}). Unexpectedly, the crystal structure reveals that the extended N terminus is involved in a domain-swapping event wherein the N terminus transverses the interface to the two neighboring monomers; *i.e.* loop1 of monomer A interacted with the protease domain of monomer C, whereas the β1 and β2 of monomer A formed parallel β-sheets with β2 of monomer B and β1 of monomer C, respectively (Fig. 3*A*). Because of the relatively low local resolution, the side chains of residues at loop1 could not be unambiguously identified. However, loop1 has extensive contact with the neighboring monomer protease domain, as revealed by detailed protein interface analysis (Fig. S4). Biochemical data demonstrated that truncation of loop1 also abrogated the *Hp*HtrA trimer into a monomer (Fig. S5*A*). The parallel β-sheets formed by two β-strands from neighboring monomers are connected by interstrand backbone hydrogen bonds. In particular, the side chain of Arg^{31} from monomer A stretched out and formed a typical salt bridge with Asp^{173} from monomer C. This intermolecular Arg^{31}-Asp^{173} salt bridge is highly conserved in all three monomers (Fig. 3*B* and Fig. S6). It is worth noting that the N-terminal domain swapping of *Hp*HtrA contributes to majority of protein–protein interfaces in *Hp*HtrA. The average interface area between two neighboring monomers in the *Hp*HtrA trimer is 1656 Å^2, which is significantly larger than that in *Ec*DegP and *Ec*DegQ. However, truncation of the N-terminal 18 residues (including loop1 and the β1 strand) and 26 residues (including loop1, the β1 strand, loop2, and the β2 strand) dramatically reduced the interface areas to 690 Å^2 and 446 Å^2, respectively (Fig. 3*C*), which is consistent with experimental results showing that truncation of the corresponding N-terminal regions causes trimer disassembly.

The data suggest that N-terminal domain swapping is important to stabilize the *Hp*HtrA homotrimer, which is distinct from other HtrA homologs. In previously reported HtrA homolog structures, including *Ec*DegP and *Ec*DegQ, formation of a homotrimer is exclusively mediated by intersubunit hydrophobic interactions involving the first α-helix and two β-strands of the protease domain rather than domain swapping (Fig. 3*D*) (23). Moreover, urea denaturation curves revealed that *Hp*HtrA and *Ec*DegQ had a denaturation midpoint of 5.0 M and 4.5 M urea, respectively (Fig. 3*E*), indicating that *Hp*HtrA is relatively more stable than *Ec*DegQ, which is consistent with the fact that *Hp*HtrA has larger intersubunit interface areas. Therefore, *Hp*HtrA represents a novel type of homotrimer of HtrA family proteases stabilized by unique N-terminal domain swapping.

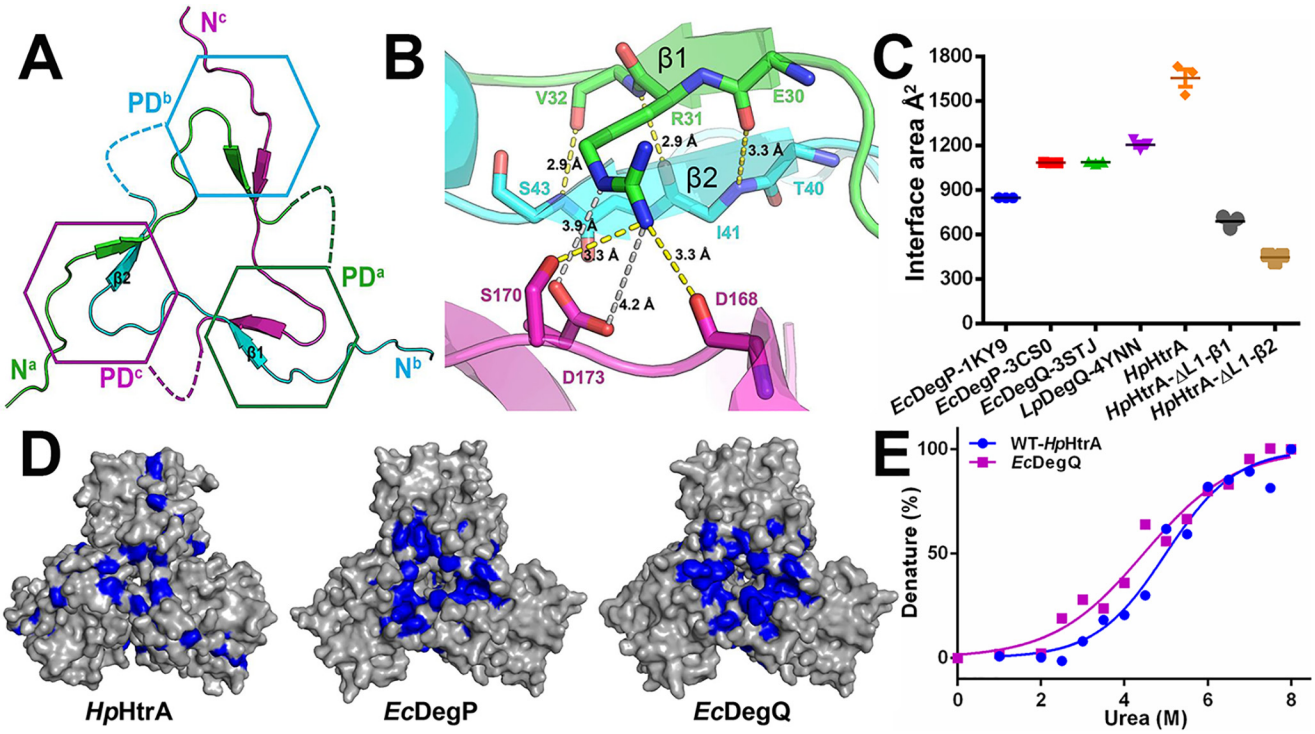

Figure 3. The N terminus stabilizes the *Hp*HtrA trimer. *A*, schematic of N-terminal domain swapping in *Hp*HtrA. The N termini of *Hp*HtrA trimer are shown as cartoons in different colors as indicated. The protease domains are presented as *hexagons*. β-Strands 1 and 2 in chain B are labeled. *B*, details of the interfaces among three different *Hp*HtrA monomers. Three *Hp*HtrA monomers are shown in different colors. Residues involved in the interactions are shown as *sticks*. Hydrogen bonds are indicated as *yellow dashed lines*. The salt bridge is shown as a *gray dashed line*. *C*, interface area analysis of HtrA family proteins. The interface areas between each pair of monomers in HtrA protein trimer were analyzed using the PDBePISA server. The abbreviated species names are as follows: *EcDegP-1KY9*, *E. coli* DegP (PDB code 1KY9); *EcDegP-3CS0*, *Escherichia coli* DegP (PDB code 3CS0); *EcDegQ-3STJ*, *E. coli* DegQ (PDB code 3STJ); *LpDegQ-4YNN*, *L. pneumophila* DegQ (PDB code 4YNN); *HpHtrA*, *H. pylori* HtrA; *HpHtrA-ΔL1-β1*, *Hp*HtrA with N-terminal loop1 and the β1 strand truncated; *HpHtrA-ΔL1-β2*, *Hp*HtrA with N-terminal loop1, the β1 strand, loop2, and the β2 strand truncated. *D*, HtrA family protein trimer interface analysis. The surfaces of trimeric *Hp*HtrA, *Ec*DegP, and *Ec*DegQ are shown in *gray*. The hydrophobic residues involved in trimer interfaces are highlighted in *blue*. *E*, urea denaturation curves of the *Hp*HtrA (*blue circles*) and *Ec*DegQ (*purple squares*).

Substrate binding triggers HpHtrA oligomer formation

It has been demonstrated that substrate binding to *Ec*DegP and *Ec*DegQ induces proteolytically active oligomer formation (18, 19, 22, 48). To examine whether *Hp*HtrA employs a similar activation mechanism, we first analyzed the *Hp*HtrA oligomeric state in the presence of β-casein, which is a well-characterized unfolded model substrate for the HtrA family (49). Similar to *Ec*DegP and *Ec*DegQ, size-exclusion chromatography analysis revealed that incubation of *Hp*HtrA with different molar equivalents of β-casein led to formation of a higher-order oligomer, *i.e.* a substrate-engaged 12-mer (*Hp*HtrA12) and 24-mer (*Hp*HtrA24) (Fig. S7*A*). The sizes of the formed complexes are dependent on the β-casein substrate concentration. At lower substrate concentration, the 12-mer is predominantly formed, whereas *Hp*HtrA24 was observed with increasing concentration of substrate.

Time-dependent analysis of the *Hp*HtrA proteolytic products by size-exclusion chromatography showed that β-casein cleavage products by *Hp*HtrA had two major groups of elution peaks, with the first peak eluted slightly later than β-casein, denoted as the primary product, and several smaller peaks eluted much later, denoted as the secondary products (Fig. 4*A*). In the course of time, the amounts of primary cleavage product were decreased, accompanied by an increase of the secondary cleavage products. The amount of *Hp*HtrA12 was also decreasing during the cleavage process, indicating that the proteolytically active *Hp*HtrA oligomer dissociated after substrate cleavage (Fig. S7*B*). In contrast, incubation of *Hp*HtrA-ΔN with β-casein yielded no detectable *Hp*HtrA oligomers or detectable cleavage products (Fig. 4*B*), suggesting that monomeric *Hp*HtrA-ΔN loses the capability to assemble into the active oligomer even in the presence of excess amount of β-casein.

The cleavage sites of E-cadherin by *Hp*HtrA were located at the linker regions of EC domains. In particular, a 21-residue P1 peptide (Ac-TGTLLLILSDVNDNAPIPEPR-COOH) derived from the cleavage site between E-cadherin domains EC4 and EC5 could bind directly to *Hp*HtrA (37). Therefore, we further investigated the binding between P1 peptide and *Hp*HtrA. No high-order oligomer complex was observed in size-exclusion chromatography when *Hp*HtrA was incubated with an excess amount of P1 peptide, which was probably due to the low binding affinity. To better characterize the interaction, atomic force microscopy (AFM) imaging experiments were carried out to capture the oligomerization state of *Hp*HtrA upon P1 peptide binding. Deposition of *Hp*HtrA alone onto freshly cleaved mica, followed by AFM imaging, resulted in distribution of the protein with a typical triangular shape, which is consistent with the trimeric form, as revealed by the crystal structure (Fig. 4*C*). Incubation of *Hp*HtrA with P1 peptide caused substantial changes in protein particle shape in AFM imaging, in which the assembly heights of complex particles are significantly larger than that of *Hp*HtrA alone, indicative of oligomerization of

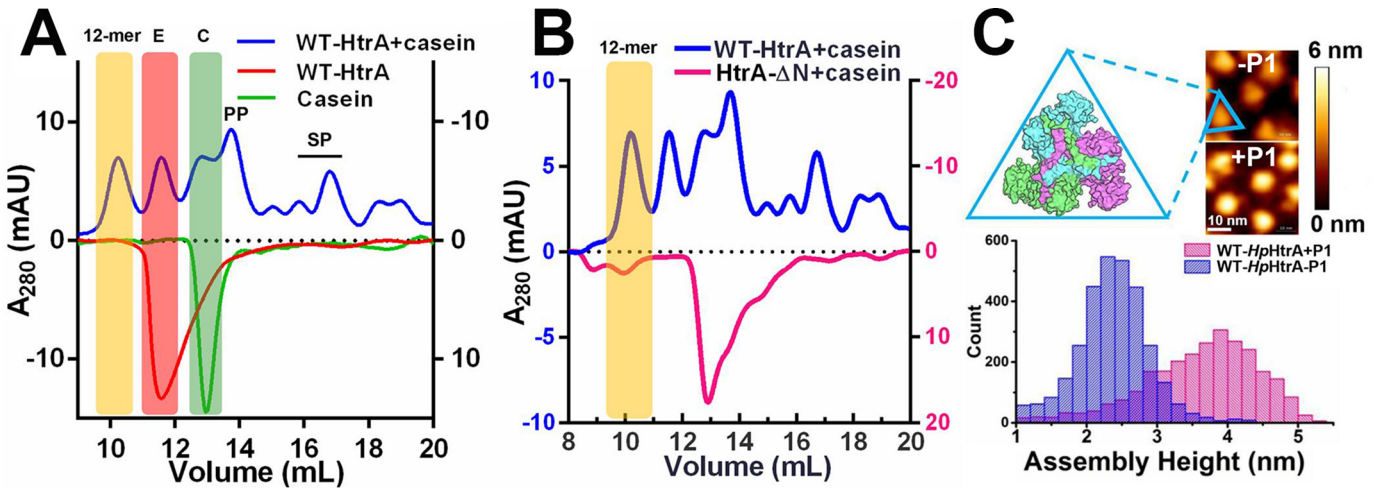

Figure 4. Substrate binding triggers formation of the *Hp*HtrA proteolytically active oligomer. *A*, size-exclusion chromatography analysis of the *Hp*HtrA oligomerization state. The elution profiles of WT *Hp*HtrA (*red*), β-casein (*green*), and the mixture of WT *Hp*HtrA and β-casein (*blue*) are shown. The abbreviated eluted fractions are as follows: *12-mer*, dodecameric WT-*Hp*HtrA complex with the substrate; *E*, trimeric WT-*Hp*HtrA; *C*, β-casein substrate; *PP*, primary digested product of β-casein; *SP*, secondary digested product of β-casein. The dodecameric *Hp*HtrA, trimeric *Hp*HtrA, and β-casein elution peaks are highlighted in *yellow*, *red*, and *green*, respectively. *mAU*, milli-absorbance units. *B*, size-exclusion chromatography profiles of WT-*Hp*HtrA (*blue*) and *Hp*HtrA-ΔN (*magenta*) incubated with β-casein substrate. The dodecameric *Hp*HtrA with the β-casein complex elution peak is highlighted in *yellow*. The WT HtrA+casein curve was reused from *A* for comparison with *Hp*HtrA-ΔN+casein. It indicates that monomeric *Hp*HtrA-ΔN cannot assemble into the active oligomer even in the presence of an excess amount of β-casein. *C*, atomic force microscopy analysis of the *Hp*HtrA oligomerization state. *Top panel*, AFM images of WT *Hp*HtrA particles without (−*P1*) and with P1 peptide (+*P1*). *Bottom panel*, assembly height distribution histograms of WT *Hp*HtrA in the absence (*blue*) and presence of P1 peptide (*magenta*).

*Hp*HtrA in the presence of P1 peptide (Fig. 4*C*). Collectively, we demonstrate that *Hp*HtrA is able to assemble and disassemble dynamically to form a proteolytically active oligomer, which is promoted by binding of an unstructured substrate.

A lysine residue of HpHtrA is important for E-cadherin cleavage

In contrast to β-casein or P1 peptide, E-cadherin is a well-folded, rigid substrate for *Hp*HtrA. To investigate the mechanism of E-cadherin cleavage by *Hp*HtrA, a protein complex structural model was built by docking E-cadherin EC1–EC2 domains to the *Hp*HtrA timer. In the docking model, the PDZ1 domains of two *Hp*HtrA monomers work as clamps to bind the EC1–EC2 domains (Fig. S8*A*). Both of the EC domains have contact interfaces with the *Hp*HtrA PDZ1 domains, which are closed to the identified PDZ1 substrate binding groove formed by β-strand A and α-helix B (28). Typically, two lysine residues, Lys^{326} and Lys^{328} from the PDZ1 domains, are proximal to the EC1 and EC2 domains in the complex model, implying that the two residues are possibly involved in EC1–EC2 domain recognition (Fig. S8*B*). To test the hypothesis, two *Hp*HtrA mutants (*Hp*HtrA-K326A and *Hp*HtrA-K328A) were purified, and their substrates cleavage activities were investigated. Both mutants maintained similar β-casein cleavage activity compared with WT-*Hp*HtrA. Intriguingly, the two mutants exhibited different cleavage activities for substrate E-cadherin. The *Hp*HtrA-K326A mutant exhibited similar E-cadherin proteolytic activity compared with WT *Hp*HtrA. In contrast, significantly attenuated E-cadherin cleavage activity was observed for the *Hp*HtrA-K328A mutant (Fig. S9). Time-course substrate cleavage assay results also confirmed that K328A mutagenesis attenuated *Hp*HtrA proteolytic activity for E-cadherin but not for β-casein (Fig. 5, *B* and *C*). The data suggest that Lys^{328} of the *Hp*HtrA PDZ1 domain is critical for E-cadherin cleavage, whereas it is dispensable for β-casein proteolysis. The complex structural model here may represent the first snapshot of the binding and recognition of E-cadherin substrate by *Hp*HtrA via the Lys^{328} residue of the PDZ1 domains, and binding of E-cadherin would further induce a conformational change of *Hp*HtrA, facilitating cleavage of bound E-cadherin at the domain linker region.

Phylogenetic analysis and cellular localization of HpHtrA

In *E. coli*, three members of the HtrA family have been identified: *Ec*DegP, *Ec*DegQ, and *Ec*DegS. The three proteases exert different bacterial physiological functions (48, 50, 51). In contrast, only one HtrA homolog has been identified in *H. pylori*, implying that *Hp*HtrA could be multifunctional in *H. pylori*. Sequence alignment of HtrA family proteins from several eukaryotic and prokaryotic species revealed that a similar extended N terminus can be found in *Campylobacter jejuni* HtrA (*Cj*HtrA), which is also an identified protease secreted by human pathogenic bacteria. Intriguingly, the N terminus of *Hp*HtrA exhibits high sequence similarity with the N-terminal region of DegS homologs, which is part of the transmembrane domain (Fig. S10). Further phylogenetic analysis of HtrA family proteins also indicates that *Hp*HtrA is more closely related to DegS than to DegP, implying a potential evolutionary relationship between DegS and *Hp*HtrA (Fig. 5*D*).

HpHtrA is a virulence factor secreted by H. pylori

*Hp*HtrA contains a signal peptide for Sec-dependent transport across the inner membrane into the periplasm (52). However, it is still unknown whether *Hp*HtrA is simultaneously transported across the out membrane when it enters the periplasm. Therefore, we investigated the cellular localization of *Hp*HtrA with an *Hp*HtrA-specific antibody. As shown in Fig. 5*E* (Fig. S11), clear *Hp*HtrA protein bands were visible in the bacterial culture medium and soluble fraction after cell lysis.

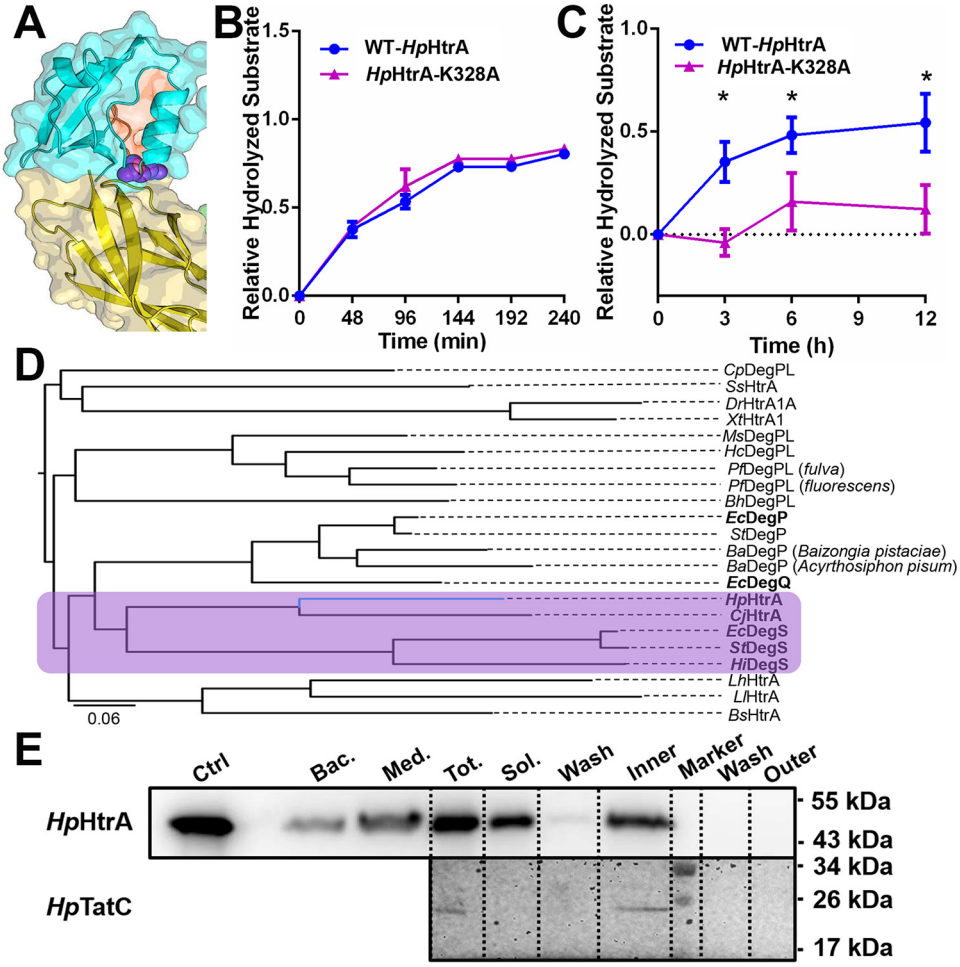

Figure 5. Substrate recognition model and phylogenetic analysis of *Hp*HtrA. *A*, details of the interfaces between the *Hp*HtrA PDZ1 domain and EC1–EC2. The peptide binding groove of the *Hp*HtrA PDZ1 domain is colored *orange*. The Lys^{328} residue involved in E-cadherin recognition is shown as *purple spheres*. *B* and *C*, time-course cleavage assay of β-casein (*B*) and N-terminal E-cadherin (*C*) by WT *Hp*HtrA and the *Hp*HtrA(K328A) mutant. The total amount of substrate is normalized as 1, and the hydrolyzed substrates are plotted against time. The experiments were performed in triplicate, and the results are shown as mean value with standard deviation. *D*, phylogenetic tree of the HtrA family. The *Hp*HtrA and DegS branches are highlighted in *purple*. The abbreviated species names and their GenBank accession numbers are as follows: *CpDegPL*, *Chlamydia pneumoniae* DegPL (Q9Z6T0); *SsHtrA*, *Synechocystis* sp. HtrA (P73354); *DrHtrA1A*, *Danio rerio* HtrA1A (Q6GMI0); *XtHtrA*, *Xenopus tropicalis* HtrA (A4IHA1); *MsDegPL*, *Marinomonas* sp. DegPL (A6VUA4); *HcDegPL*, *H. chejuensis* DegPL (Q2SL36); *PfDegPL (fulva)*, *Pseudomonas fulva* DegPL (F6AA62); *PfDegPL (fluorescens)*, *Pseudomonas fluorescens* DegPL (Q4KGQ4); *BhDegPL*, *Bartonella henselae* DegPL (P54925); *EcDegP*, *E. coli* DegP (P0C0V0); *StDegP*: *Salmonella enterica* serovar Typhimurium DegP (P26982); *BaDegP (Baizongia pistaciae)*, *Buchnera aphidicola* subsp. *Baizongia pistaciae* DegP (Q89AP5); *BaDegP (Acyrthosiphon pisum)*, *B. aphidicola* subsp. *Acyrthosiphon pisum* DegP (P57322); *EcDegQ*, *E. coli* DegQ (P39099); *HpHtrA*, *H. pylori* HtrA (G2J5T2); *CjHtrA*, *C. jejuni* HtrA (A7H2F1); *EcDegS*, *E. coli* DegS (P0AEE3); *StDegS*, *S. enterica* Typhimurium DegS (D0ZY51); *HiDegS*: *Haemophilus influenzae* DegS (P44947); *LhHtrA*, *Lactobacillus helveticus* HtrA (Q9Z4H7); *LlHtrA*, *Lactococcus lactis* HtrA (A2RNT9); *BsHtrA*: *Bacillus subtilis* HtrA (P39668). *E*, cellular location analysis of *Hp*HtrA; Western blot analysis of *Hp*HtrA in different separation fractions. *Ctrl*, purified *Hp*HtrA protein; *Bac.*, bacterial pellet; *Med.*, extracellular medium; *Tot.*, total protein after bacterial lysis; *Sol.*, soluble protein after bacterial lysis; *Wash*, wash of pellet after cell lysis; *Inner*, inner membrane protein; *Outer*, outer membrane protein; *HpTatC*, twin-arginine translocation protein C, an inner membrane protein of *H. pylori*. *Hp*TatC was observed in the total lysate and inner membrane fractions.

The soluble fraction should include *Hp*HtrA from both the bacterial cytoplasm and periplasm. Surprisingly, substantial amounts of *Hp*HtrA were also identified in the inner membrane fraction, implying that *Hp*HtrA might directly anchor to the inner membrane or bind tightly to an inner-membrane protein. The results demonstrate that the *H. pylori* periplasm and inner membrane may serve as temporary reservoirs for *Hp*HtrA before its extracellular secretion.

Discussion

It is well established that *H. pylori* translocates a virulence factor, CagA, into the gastric epithelial cell cytoplasm via a type IV secretion system (53, 54). Such a process depends on interaction of the bacterial type IV secretion system with the host cell surface $\alpha_5\beta_1$ receptor (55–57). Recent studies demonstrated that *H. pylori* utilizes a novel secreted serine protease, HtrA, to cleave the host Occludin, Claudin-8, as well as E-cadherin proteins, which breaks down the E-cadherin–based adherens junctions and tight junctions between gastric epithelial cells to disintegrate the epithelial barrier. After cleavage, *H. pylori* can efficiently enter the intercellular space and interact with the exposed $\alpha_5\beta_1$ receptors for virulence factor translocation (11, 29, 37). The HtrA protein was initially identified as a protease, functioning in the bacterial periplasmic space for protein quality control. Recent studies demonstrated that HtrA-mediated host cell E-cadherin cleavage is a prevalent pathogenic mechanism for multiple Gram-negative bacterial species, indicating that bacterial

HtrA could serve as an attractive target for the design of antibacterial agents (30, 38, 39).

Here we determined the crystal structure of *H. pylori* HtrA protease, which possesses an extended N terminus different from other homologs. In the crystal structure, three *Hp*HtrA monomeric molecules assemble into a new type of trimer via unique N-terminal domain swapping. Importantly, the *Hp*HtrA trimer is mainly stabilized by N-terminal domain swapping. This assembly pattern is distinct from that of the *E. coli* homologs DegP and DegQ, both of which are stabilized by hydrophobic interactions of the protease domains. Truncation of the N terminus completely abrogated *Hp*HtrA trimer formation, leading to monomeric *Hp*HtrA without detectable protease activity, indicative of the essential role of the N terminus. A recent study of *Hp*HtrA demonstrated that autocleavage of the *Hp*HtrA N terminus abolished *Hp*HtrA secretion and protease activity, which is consistent with our protein structure data (58). Although it is still unknown why *Hp*HtrA adopts such a unique mechanism for protein trimer assembly, one plausible explanation is that larger intersubunit interface areas contributed by domain swapping enhance *Hp*HtrA trimer stability so that *Hp*HtrA can sustain protease activity after secretion into the hostile gastric niche (59). Therefore, targeting the N terminus to abolish *Hp*HtrA trimer formation may represent a new potential anti-*H. pylori* strategy.

Similar to other HtrA homologs, *Hp*HtrA could assemble into a proteolytically active oligomer in the presence of β-casein substrate. Similar assembly was also observed when *Hp*HtrA was incubated with P1 peptide, which is derived from the E-cadherin cleavage site. However, *Hp*HtrA oligomerization is unlikely to happen when *Hp*HtrA binds to the E-cadherin ectodomain. Unlike unstructured β-casein or peptide, E-cadherin is a rigid protein with a well-folded structure, which could prevent the higher multimer active cage formation of *Hp*HtrA. Previous studies demonstrated that *Ec*DegP oligomeric cage assembly is not required for its proteolytic activation (60). It would not be surprising if *Hp*HtrA could cleave E-cadherin in the trimeric form. Therefore, the recognition and cleavage mechanism of E-cadherin by *Hp*HtrA should be different from that of β-casein. Indeed, our biochemical studies identified that Lys^{328} of *Hp*HtrA was indispensable for E-cadherin cleavage but not for β-casein.

Although *Hp*HtrA contains two PDZ domains similar to *Ec*DegP and *Ec*DegQ, phylogenetic analysis reveals a closer evolutionary relationship between *Hp*HtrA and *Ec*DegS. *Ec*DegS is a serine protease anchored on the *E. coli* inner membrane and involved in the cellular response to extracytoplasmic stress via activation of the *E. coli* σ factor σ^E (61). Cellular localization analysis revealed that a substantial amount of *Hp*HtrA was also identified in the bacterial inner membrane. Although it is unknown how *Hp*HtrA is attached to the inner membrane, it is possible that *H. pylori* adopts a strategy to preserve *Hp*HtrA so that export of the virulence factor could occur by a triggered mechanism, which avoids unnecessary secretion. Therefore, it would be interesting to further investigate whether the cellular localization of *Hp*HtrA is functionally relevant.

Conclusion

In summary, we report the first crystal structure of the *H. pylori* HtrA trimer stabilized by unique N-terminal domain swapping, which represents an unprecedented novel assembly of HtrA family proteases. The N terminus of HtrA from *H. pylori* is also indispensable for its protease activity. The molecular mechanism of how *Hp*HtrA recognizes and cleaves E-cadherin was elucidated based on a structural model that is distinct from that of the conventional substrate β-casein. Given that *Hp*HtrA is a promising target for the design of anti-*H. pylori* agents, the structure we report here could facilitate the development of a new type of anti-*H. pylori* agents by targeting HtrA both at the active site and N terminus.

Experimental procedures

Protein expression and purification

Details regarding expression and purification of *H. pylori* HtrA proteins can be found in the supporting Methods. In brief, N-terminal His-tagged *H. pylori* WT or mutant HtrA proteins lacking the signal peptide sequence were expressed in the *E. coli BL21* (DE3) strain and purified by nickel affinity chromatography followed by gel filtration. Recombinant proteins were pooled and stored at −80 °C. All the PCR primers were listed in Table S1.

Protein crystallization and structure determination

Crystals of full-length *Hp*HtrA were obtained by sitting drop diffusion at 20 °C and mixing equal volumes of the protein and the reservoir solution, consisting of 2.1 M DL-malic acid, and 0.1 M HEPES (pH 7.0). For *Hp*HtrA-ΔPDZ2, crystals were obtained similarly, with the reservoir solution containing 20% PEG 1500, 0.1 M HEPES (pH 7.5), and 0.2 M proline. Crystals were cryoprotected with reservoir solution supplemented with 10% glycerol and flash-frozen in liquid nitrogen. Diffraction data were performed at the Shanghai Synchrotron Radiation Facility (Shanghai, China) using beamlines 17B, 17U1, and 19U1. Raw data images were processed with HKL2000 (62). Molecular replacement solution was obtained from the PHENIX program using *E. coli* DegP (PDB code 1KY9) as a search model (63). Subsequent model building and refinement were carried out in COOT (64) and PHENIX (Table S2). The figures were prepared using PyMOL (Schrödinger, LLC).

HpHtrA proteolytic activity

*Hp*HtrA proteolytic assays were performed as described previously (65). For the time-course β-casein cleavage assay, 40 nM WT *Hp*HtrA or mutants was incubated with 3 μg of β-casein in reaction buffer (20 mM Tris-HCl (pH 7.5), 250 mM NaCl, and 1 mM DTT) at 37 °C. At the indicated times, aliquots of the reactions were removed for SDS-PAGE analysis. For the E-cadherin cleavage assay, ~0.8 μM WT *Hp*HtrA or mutants was incubated with 50 ng of the N-terminal domain of E-cadherin in reaction buffer for 16 h at 37 °C. The remaining substrates were blotted with an antibody to E-cadherin. The SDS-PAGE and Western blot band intensities were quantified using ImageJ software (66).

Atomic force microscopy imaging

AFM imaging was carried out in QI mode in liquid with a NanoWizard 4 microscope (JPK Instruments AG) equipped with SNL-10 cantilevers (Bruker Probes). Square images of 256 × 256 pixels were collected with a scan size of 500 nm and a set point of 300 pN. For each experiment, ~20 μl of *Hp*HtrA protein samples (0.01 mg/ml) in the absence or presence of P1 peptide was added onto freshly cleaved mica and allowed to absorb for 15 min. After that, the mica surface was rinsed and submerged in Tris buffer (400 mM Tris-HCl (pH 7.4) and 100 mM NaCl).

Size-exclusion chromatography analysis

Size-exclusion chromatography was performed with a Tricorn Superdex 200 Increase 10/300 GL column (GE Healthcare) at 4 °C. The column was calibrated with a gel filtration calibration kit (GE Healthcare) and pre-equilibrated with gel filtration buffer (20 mM Tris-HCl (pH 7.5), 250 mM NaCl, and 1 mM DTT). For oligomerization state analysis, 100-μl samples containing 40 μM WT *Hp*HtrA or mutants were injected into the column. For substrate-triggered oligomer formation, ~100 μl of protein mixtures containing 40 mM *Hp*HtrA and 160 mM β-casein or E-cadherin EC1-EC2 domain was incubated on ice for the indicated time before loading onto the column.

Structure model of the HpHtrA and E-cadherin complex

An *Hp*HtrA trimer structure model with three intact PDZ1 domains was generated using chain C of the *Hp*HtrA-ΔPDZ2 structure (PDB code 5Y28) as a template. The protein complex structure was built by docking the structure of the human E-cadherin EC1–2 domain (PDB code 4ZT1) to the *Hp*HtrA trimer using the ESCHER protein–protein automatic docking system with default parameters (67). The structure with the lowest energy was selected as the complex model.

Circular dichroism

CD spectra were recorded at ambient temperature on a JASCO J-810 spectrophotometer using a quartz cuvette with a path length of 0.1 cm. Urea denaturation experiments were performed as described previously (68). In brief, urea gradients were added to 20 μM WT *Hp*HtrA and *Ec*DegQ in 10 mM Tris–H_2SO_4 buffer supplemented with 100 mM $NaSO_4$ (pH 7.5). After equilibrating overnight at 4 °C, CD spectra were recorded between 200 and 270 nm with an average of three scans. The absorption at 220 nm was used to characterize the unfolding state of the protein.

Sequence alignment and phylogeny analysis

HtrA family protein sequence alignment and the phylogenetic tree were done using the MAFFT online program (version 7) with default options (https://mafft.cbrc.jp/alignment/server/).[4] All protein sequences were obtained from the UniProt database, and signal peptide sequences were removed manually.

[4] Please note that the JBC is not responsible for the long-term archiving and maintenance of this site or any other third party–hosted site.

Analysis of the cellular location of HpHtrA

The separation of inner and outer membranes was carried out according to the method described by Doig and Trust (69) with minor modifications. Details of the experiments are described in the supporting Methods. All cellular fractions were analyzed by Western blotting using an *Hp*HtrA-specific antibody.

Accession codes

The coordinates for full-length *Hp*HtrA and *Hp*HtrA-ΔPDZ2 have been deposited in the PDB with accession codes 5Y2D and 5Y28, respectively.

Author contributions—Z. Z., Q. H., X. T., G. S., P. Z., H. L., and H. S. data curation; Z. Z. and Q. H. formal analysis; Z. Z. and Q. H. writing-original draft; Q. H. and X. T. validation; Q. H. methodology; P. Z., H. S., and W. X. supervision; H. L., H. S., and W. X. writing-review and editing; H. S. and W. X. funding acquisition; W. X. conceptualization; W. X. investigation; W. X. project administration.

Acknowledgments—We thank the staff of the BL17B, BL17U1, and BL19U1 beamlines of the Shanghai Synchrotron Radiation Facility for assistance with data collection.

References

1. Levy, S. B., and Marshall, B. (2004) Antibacterial resistance worldwide: causes, challenges and responses. *Nat. Med.* **10,** S122–S129 CrossRef Medline
2. Dickey, S. W., Cheung, G. Y. C., and Otto, M. (2017) Different drugs for bad bugs: antivirulence strategies in the age of antibiotic resistance. *Nat. Rev. Drug Discov.* **16,** 457–471 CrossRef Medline
3. Rasko, D. A., and Sperandio, V. (2010) Anti-virulence strategies to combat bacteria-mediated disease. *Nat. Rev. Drug Discov.* **9,** 117–128 CrossRef Medline
4. Polk, D. B., and Peek, R. M., Jr. (2010) *Helicobacter pylori*: gastric cancer and beyond. *Nat. Rev. Cancer* **10,** 403–414 CrossRef Medline
5. Hatakeyama, M. (2004) Oncogenic mechanisms of the *Helicobacter pylori* CagA protein. *Nat. Rev. Cancer* **4,** 688–694 CrossRef Medline
6. Foegeding, N. J., Caston, R. R., McClain, M. S., Ohi, M. D., and Cover, T. L. (2016) An overview of *Helicobacter pylori* VacA toxin biology. *Toxins* **8,** E173 Medline
7. Mégraud, F., Neman-Simha, V., and Brügmann, D. (1992) Further evidence of the toxic effect of ammonia produced by *Helicobacter pylori* urease on human epithelial cells. *Infect. Immun.* **60,** 1858–1863 Medline
8. Yang, X., Koohi-Moghadam, M., Wang, R., Chang, Y. Y., Woo, P. C. Y., Wang, J., Li, H., and Sun, H. (2018) Metallochaperone UreG serves as a new target for design of urease inhibitor: a novel strategy for development of antimicrobials. *PLoS Biol.* **16,** e2003887 CrossRef Medline
9. Tarsia, C., Danielli, A., Florini, F., Cinelli, P., Ciurli, S., and Zambelli, B. (2018) Targeting *Helicobacter pylori* urease activity and maturation: in-cell high-throughput approach for drug discovery. *Biochim. Biophys. Acta Gen. Subj.* **1862,** 2245–2253 CrossRef Medline
10. Rieder, G., Fischer, W., and Haas, R. (2005) Interaction of *Helicobacter pylori* with host cells: function of secreted and translocated molecules. *Curr. Opin. Microbiol.* **8,** 67–73 CrossRef Medline
11. Tegtmeyer, N., Wessler, S., Necchi, V., Rohde, M., Harrer, A., Rau, T. T., Asche, C. I., Boehm, M., Loessner, H., Figueiredo, C., Naumann, M., Palmisano, R., Solcia, E., Ricci, V., and Backert, S. (2017) *Helicobacter pylori* employs a unique basolateral type IV secretion mechanism for CagA delivery. *Cell Host Microbe* **22,** 552–560.e5 CrossRef Medline
12. Gottesman, S., Wickner, S., and Maurizi, M. R. (1997) Protein quality control: triage by chaperones and proteases. *Genes Dev.* **11,** 815–823 CrossRef Medline

13. Ingmer, H., and Brøndsted, L. (2009) Proteases in bacterial pathogenesis. *Res. Microbiol.* **160,** 704–710 CrossRef Medline
14. Frees, D., Brondsted, L., and Ingmer, H. (2013) Bacterial proteases and virulence. *Subcell. Biochem.* **66,** 161–192 CrossRef Medline
15. Kennedy, M. B. (1995) Origin of PDZ (DHR, GLGF) domains. *Trends Biochem. Sci.* **20,** 350 CrossRef Medline
16. Sohn, J., Grant, R. A., and Sauer, R. T. (2007) Allosteric activation of DegS, a stress sensor PDZ protease. *Cell* **131,** 572–583 CrossRef Medline
17. Suzuki, Y., Imai, Y., Nakayama, H., Takahashi, K., Takio, K., and Takahashi, R. (2001) A serine protease, HtrA2, is released from the mitochondria and interacts with XIAP, inducing cell death. *Mol. Cell* **8,** 613–621 CrossRef Medline
18. Jiang, J., Zhang, X., Chen, Y., Wu, Y., Zhou, Z. H., Chang, Z., and Sui, S.-F. (2008) Activation of DegP chaperone-protease via formation of large cage-like oligomers upon binding to substrate proteins. *Proc. Natl. Acad. Sci. U.S.A.* **105,** 11939–11944 CrossRef Medline
19. Bai, X. C., Pan, X. J., Wang, X. J., Ye, Y. Y., Chang, L. F., Leng, D., Lei, J., and Sui, S. F. (2011) Characterization of the structure and function of *Escherichia coli* DegQ as a representative of the DegQ-like proteases of bacterial HtrA family proteins. *Structure* **19,** 1328–1337 CrossRef Medline
20. Zhang, L., Wang, X., Fan, F., Wang, H. W., Wang, J., Li, X., and Sui, S. F. (2017) Cryo-EM structure of Nma111p, a unique HtrA protease composed of two protease domains and four PDZ domains. *Cell Res.* **27,** 582–585 CrossRef Medline
21. Kim, D. Y., and Kim, K. K. (2005) Structure and function of HtrA family proteins, the key players in protein quality control. *J. Biochem. Mol. Biol.* **38,** 266–274 Medline
22. Krojer, T., Sawa, J., Schäfer, E., Saibil, H. R., Ehrmann, M., and Clausen, T. (2008) Structural basis for the regulated protease and chaperone function of DegP. *Nature* **453,** 885–890 CrossRef Medline
23. Krojer, T., Garrido-Franco, M., Huber, R., Ehrmann, M., and Clausen, T. (2002) Crystal structure of DegP (HtrA) reveals a new protease-chaperone machine. *Nature* **416,** 455–459 CrossRef Medline
24. Maurizi, M. R. (2002) Love it or cleave it: tough choices in protein quality control. *Nat. Struct. Biol.* **9,** 410–412 CrossRef Medline
25. Shen, Q.-T., Bai, X.-C., Chang, L.-F., Wu, Y., Wang, H.-W., and Sui, S.-F. (2009) Bowl-shaped oligomeric structures on membranes as DegP's new functional forms in protein quality control. *Proc. Natl. Acad. Sci. U.S.A.* **106,** 4858–4863 CrossRef Medline
26. Kim, S., Grant, R. A., and Sauer, R. T. (2011) Covalent linkage of distinct substrate degrons controls assembly and disassembly of DegP proteolytic cages. *Cell* **145,** 67–78 CrossRef Medline
27. Clausen, T., Southan, C., and Ehrmann, M. (2002) The HtrA family of proteases: implications for protein composition and cell fate. *Mol. Cell* **10,** 443–455 CrossRef Medline
28. Clausen, T., Kaiser, M., Huber, R., and Ehrmann, M. (2011) HTRA proteases: regulated proteolysis in protein quality control. *Nat. Rev. Mol. Cell Biol.* **12,** 152–162 CrossRef Medline
29. Hoy, B., Löwer, M., Weydig, C., Carra, G., Tegtmeyer, N., Geppert, T., Schröder, P., Sewald, N., Backert, S., Schneider, G., and Wessler, S. (2010) *Helicobacter pylori* HtrA is a new secreted virulence factor that cleaves E-cadherin to disrupt intercellular adhesion. *EMBO Rep.* **11,** 798–804 CrossRef Medline
30. Hoy, B., Geppert, T., Boehm, M., Reisen, F., Plattner, P., Gadermaier, G., Sewald, N., Ferreira, F., Briza, P., Schneider, G., Backert, S., and Wessler, S. (2012) Distinct roles of secreted HtrA proteases from gram-negative pathogens in cleaving the junctional protein and tumor suppressor E-cadherin. *J. Biol. Chem.* **287,** 10115–10120 CrossRef Medline
31. Boehm, M., Hoy, B., Rohde, M., Tegtmeyer, N., Bæk, K. T., Oyarzabal, O. A., Brøndsted, L., Wessler, S., and Backert, S. (2012) Rapid paracellular transmigration of *Campylobacter jejuni* across polarized epithelial cells without affecting TER: role of proteolytic-active HtrA cleaving E-cadherin but not fibronectin. *Gut Pathog.* **4,** 3 CrossRef Medline
32. Löwer, M., Weydig, C., Metzler, D., Reuter, A., Starzinski-Powitz, A., Wessler, S., and Schneider, G. (2008) Prediction of extracellular proteases of the human pathogen *Helicobacter pylori* reveals proteolytic activity of the Hp1018/19 protein HtrA. *PLoS ONE* **3,** e3510 CrossRef Medline
33. Skorko-Glonek, J., Zurawa-Janicka, D., Koper, T., Jarzab, M., Figaj, D., Glaza, P., and Lipinska, B. (2013) HtrA protease family as therapeutic targets. *Curr. Pharm. Des.* **19,** 977–1009 Medline
34. Olofsson, A., Vallström, A., Petzold, K., Tegtmeyer, N., Schleucher, J., Carlsson, S., Haas, R., Backert, S., Wai, S. N., Gröbner, G., and Arnqvist, A. (2010) Biochemical and functional characterization of *Helicobacter pylori* vesicles. *Mol. Microbiol.* **77,** 1539–1555 CrossRef Medline
35. Niessen, C. M. (2007) Tight junctions/adherens junctions: basic structure and function. *J. Invest. Dermatol.* **127,** 2525–2532 CrossRef Medline
36. Niessen, C. M., Leckband, D., and Yap, A. S. (2011) Tissue organization by cadherin adhesion molecules: dynamic molecular and cellular mechanisms of morphogenetic regulation. *Physiol. Rev.* **91,** 691–731 CrossRef Medline
37. Schmidt, T. P., Perna, A. M., Fugmann, T., Böhm, M., Hiss, J., Haller, S., Götz, C., Tegtmeyer, N., Hoy, B., Rau, T. T., Neri, D., Backert, S., Schneider, G., and Wessler, S. (2016) Identification of E-cadherin signature motifs functioning as cleavage sites for *Helicobacter pylori* HtrA. *Sci. Rep.* **6,** 23264 CrossRef Medline
38. Perna, A. M., Reisen, F., Schmidt, T. P., Geppert, T., Pillong, M., Weisel, M., Hoy, B., Simister, P. C., Feller, S. M., Wessler, S., and Schneider, G. (2014) Inhibiting *Helicobacter pylori* HtrA protease by addressing a computationally predicted allosteric ligand binding site. *Chem. Sci.* **5,** 3583–3590 CrossRef Medline
39. Perna, A. M., Rodrigues, T., Schmidt, T. P., Böhm, M., Stutz, K., Reker, D., Pfeiffer, B., Altmann, K. H., Backert, S., Wessler, S., and Schneider, G. (2015) Fragment-based *de novo* design reveals a small-molecule inhibitor of *Helicobacter Pylori* HtrA. *Angew. Chem. Int. Ed. Engl.* **54,** 10244–10248 CrossRef Medline
40. Salama, N. R., Shepherd, B., and Falkow, S. (2004) Global transposon mutagenesis and essential gene analysis of *Helicobacter pylori*. *J. Bacteriol.* **186,** 7926–7935 CrossRef Medline
41. Tegtmeyer, N., Moodley, Y., Yamaoka, Y., Pernitzsch, S. R., Schmidt, V., Traverso, F. R., Schmidt, T. P., Rad, R., Yeoh, K. G., Bow, H., Torres, J., Gerhard, M., Schneider, G., Wessler, S., and Backert, S. (2016) Characterisation of worldwide *Helicobacter pylori* strains reveals genetic conservation and essentiality of serine protease HtrA. *Mol. Microbiol.* **99,** 925–944 CrossRef Medline
42. Raju, R. M., Goldberg, A. L., and Rubin, E. J. (2012) Bacterial proteolytic complexes as therapeutic targets. *Nat. Rev. Drug Discov.* **11,** 777–789 CrossRef Medline
43. Jomaa, A., Damjanovic, D., Leong, V., Ghirlando, R., Iwanczyk, J., and Ortega, J. (2007) The inner cavity of *Escherichia coli* DegP protein is not essential for molecular chaperone and proteolytic activity. *J. Bacteriol.* **189,** 706–716 CrossRef Medline
44. Iwanczyk, J., Damjanovic, D., Kooistra, J., Leong, V., Jomaa, A., Ghirlando, R., and Ortega, J. (2007) Role of the PDZ domains in *Escherichia coli* DegP protein. *J. Bacteriol.* **189,** 3176–3186 CrossRef Medline
45. Wilken, C., Kitzing, K., Kurzbauer, R., Ehrmann, M., and Clausen, T. (2004) Crystal structure of the DegS stress sensor: how a PDZ domain recognizes misfolded protein and activates a protease. *Cell* **117,** 483–494 CrossRef Medline
46. Skórko-Glonek, J., Zurawa, D., Tanfani, F., Scirè, A., Wawrzynów, A., Narkiewicz, J., Bertoli, E., and Lipińska, B. (2003) The N-terminal region of HtrA heat shock protease from *Escherichia coli* is essential for stabilization of HtrA primary structure and maintaining of its oligomeric structure. *Biochim. Biophys. Acta* **1649,** 171–182 CrossRef Medline
47. Krojer, T., Sawa, J., Huber, R., and Clausen, T. (2010) HtrA proteases have a conserved activation mechanism that can be triggered by distinct molecular cues. *Nat. Struct. Mol. Biol.* **17,** 844–852 CrossRef Medline
48. Sawa, J., Malet, H., Krojer, T., Canellas, F., Ehrmann, M., and Clausen, T. (2011) Molecular adaptation of the DegQ protease to exert protein quality control in the bacterial cell envelope. *J. Biol. Chem.* **286,** 30680–30690 CrossRef Medline
49. Swaisgood, H. E. (1993) Review and update of casein chemistry. *J. Dairy Sci.* **76,** 3054–3061 CrossRef Medline
50. Strauch, K. L., and Beckwith, J. (1988) An *Escherichia coli* mutation preventing degradation of abnormal periplasmic proteins. *Proc. Natl. Acad. Sci. U.S.A.* **85,** 1576–1580 CrossRef Medline

51. Walsh, N. P., Alba, B. M., Bose, B., Gross, C. A., and Sauer, R. T. (2003) OMP peptide signals initiate the envelope-stress response by activating DegS protease via relief of inhibition mediated by its PDZ domain. *Cell* **113,** 61–71 CrossRef Medline
52. Gloeckl, S., Ong, V. A., Patel, P., Tyndall, J. D., Timms, P., Beagley, K. W., Allan, J. A., Armitage, C. W., Turnbull, L., Whitchurch, C. B., Merdanovic, M., Ehrmann, M., Powers, J. C., Oleksyszyn, J., Verdoes, M., Bogyo, M., and Huston, W. M. (2013) Identification of a serine protease inhibitor which causes inclusion vacuole reduction and is lethal to *Chlamydia trachomatis*. *Mol. Microbiol.* **89,** 676–689 CrossRef Medline
53. Backert, S., and Selbach, M. (2008) Role of type IV secretion in *Helicobacter pylori* pathogenesis. *Cell Microbiol.* **10,** 1573–1581 CrossRef Medline
54. Grohmann, E., Christie, P. J., Waksman, G., and Backert, S. (2018) Type IV secretion in Gram-negative and Gram-positive bacteria. *Mol. Microbiol.* **107,** 455–471 Medline
55. Kwok, T., Zabler, D., Urman, S., Rohde, M., Hartig, R., Wessler, S., Misselwitz, R., Berger, J., Sewald, N., König, W., and Backert, S. (2007) *Helicobacter* exploits integrin for type IV secretion and kinase activation. *Nature* **449,** 862–866 CrossRef Medline
56. Bonsor, D. A., Pham, K. T., Beadenkopf, R., Diederichs, K., Haas, R., Beckett, D., Fischer, W., and Sundberg, E. J. (2015) Integrin engagement by the helical RGD motif of the *Helicobacter pylori* CagL protein is regulated by pH-induced displacement of a neighboring helix. *J. Biol. Chem.* **290,** 12929–12940 CrossRef Medline
57. Kaplan-Türköz, B., Jiménez-Soto, L. F., Dian, C., Ertl, C., Remaut, H., Louche, A., Tosi, T., Haas, R., and Terradot, L. (2012) Structural insights into *Helicobacter pylori* oncoprotein CagA interaction with β1 integrin. *Proc. Natl. Acad. Sci. U.S.A.* **109,** 14640–14645 CrossRef Medline
58. Albrecht, N., Tegtmeyer, N., Sticht, H., Skórko-Glonek, J., and Backert, S. (2018) Amino-terminal processing of *Helicobacter pylori* serine protease HtrA: role in oligomerization and activity regulation. *Front. Microbiol.* **9,** 642 CrossRef Medline
59. Hoy, B., Brandstetter, H., and Wessler, S. (2013) The stability and activity of recombinant *Helicobacter pylori* HtrA under stress conditions. *J. Basic Microbiol.* **53,** 402–409 CrossRef Medline
60. Kim, S., and Sauer, R. T. (2012) Cage assembly of DegP protease is not required for substrate-dependent regulation of proteolytic activity or high-temperature cell survival. *Proc. Natl. Acad. Sci. U.S.A.* **109,** 7263–7268 CrossRef Medline
61. Alba, B. M., Zhong, H. J., Pelayo, J. C., and Gross, C. A. (2001) degS (hhoB) is an essential *Escherichia coli* gene whose indispensable function is to provide σE activity. *Mol. Microbiol.* **40,** 1323–1333 CrossRef Medline
62. Otwinowski, Z., and Minor, W. (1997) Processing of X-ray diffraction data collected in oscillation mode. *Methods Enzymol.* **276,** 307–326 CrossRef Medline
63. Adams, P. D., Afonine, P. V., Bunkóczi, G., Chen, V. B., Davis, I. W., Echols, N., Headd, J. J., Hung, L. W., Kapral, G. J., Grosse-Kunstleve, R. W., McCoy, A. J., Moriarty, N. W., Oeffner, R., Read, R. J., Richardson, D. C., *et al.* (2010) PHENIX: a comprehensive Python-based system for macromolecular structure solution. *Acta Crystallogr. D Biol. Crystallogr.* **66,** 213–221 CrossRef Medline
64. Emsley, P., Lohkamp, B., Scott, W. G., and Cowtan, K. (2010) Features and development of Coot. *Acta Crystallogr. D Biol. Crystallogr.* **66,** 486–501 CrossRef Medline
65. Schmidt, T. P., Goetz, C., Huemer, M., Schneider, G., and Wessler, S. (2016) Calcium binding protects E-cadherin from cleavage by *Helicobacter pylori* HtrA. *Gut Pathog.* **8,** 29 CrossRef Medline
66. Schneider, C. A., Rasband, W. S., and Eliceiri, K. W. (2012) NIH Image to ImageJ: 25 years of image analysis. *Nat. Methods* **9,** 671–675 CrossRef Medline
67. Ausiello, G., Cesareni, G., and Helmer-Citterich, M. (1997) ESCHER: a new docking procedure applied to the reconstruction of protein tertiary structure. *Proteins* **28,** 556–567 CrossRef Medline
68. Iwig, J. S., Leitch, S., Herbst, R. W., Maroney, M. J., and Chivers, P. T. (2008) Ni(II) and Co(II) Sensing by *Escherichia coli* RcnR. *J. Am. Chem. Soc.* **130,** 7592–7606 CrossRef Medline
69. Doig, P., and Trust, T. J. (1994) Identification of surface-exposed outer membrane antigens of *Helicobacter pylori*. *Infect. Immun.* **62,** 4526–4533 Medline

The unique trimeric assembly of the virulence factor HtrA from *Helicobacter pylori* occurs via N-terminal domain swapping

Zhemin Zhang, Qi Huang, Xuan Tao, Guobing Song, Peng Zheng, Hongyan Li, Hongzhe Sun and Wei Xia

J. Biol. Chem. 2019, 294:7990-8000.
doi: 10.1074/jbc.RA119.007387 originally published online April 1, 2019